AD-A138 685 SPECTROSCOPIC MEASUREMENTS OF THE LASER-HANE PLASMA(U) 1/1
NAVAL RESEARCH LAB WASHINGTON DC E A MCLEAN ET AL.
17 FEB 84 NRL-MR-5274

UNCLASSIFIED F/G 14/2 NL

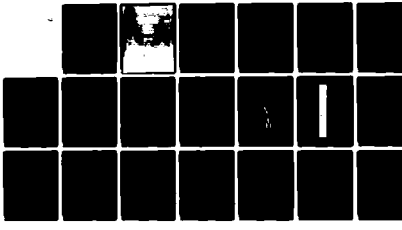

END
DATE FILMED
4 84
DTIC

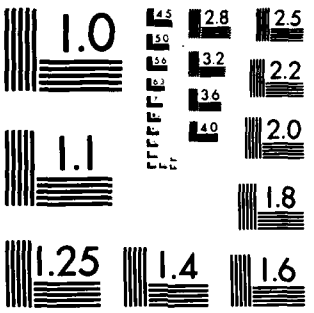

AD-A138685

SECURITY CLASSIFICATION OF THIS PAGE

## REPORT DOCUMENTATION PAGE

| | |
|---|---|
| 1a. REPORT SECURITY CLASSIFICATION<br>UNCLASSIFIED | 1b. RESTRICTIVE MARKINGS |
| 2a. SECURITY CLASSIFICATION AUTHORITY | 3. DISTRIBUTION/AVAILABILITY OF REPORT<br>Approved for public release; distribution unlimited. |
| 2b. DECLASSIFICATION/DOWNGRADING SCHEDULE | |
| 4. PERFORMING ORGANIZATION REPORT NUMBER(S)<br>NRL Memorandum Report 5274 | 5. MONITORING ORGANIZATION REPORT NUMBER(S) |
| 6a. NAME OF PERFORMING ORGANIZATION<br>Naval Research Laboratory<br>6b. OFFICE SYMBOL (If applicable) | 7a. NAME OF MONITORING ORGANIZATION |
| 6c. ADDRESS (City, State and ZIP Code)<br>Washington, DC 20375 | 7b. ADDRESS (City, State and ZIP Code) |
| 8a. NAME OF FUNDING/SPONSORING ORGANIZATION<br>Defense Nuclear Agency<br>8b. OFFICE SYMBOL (If applicable) | 9. PROCUREMENT INSTRUMENT IDENTIFICATION NUMBER |
| 8c. ADDRESS (City, State and ZIP Code)<br>Washington, DC 20305 | 10. SOURCE OF FUNDING NOS.<br>PROGRAM ELEMENT NO. 62715H; PROJECT NO.; TASK NO.; WORK UNIT NO. 47-1606-0-4 |
| 11. TITLE (Include Security Classification) SPECTROSCOPIC MEASUREMENTS OF THE LASER-HANE PLASMA | |
| 12. PERSONAL AUTHOR(S)<br>E.A. McLean, J.A. Stamper, H.R. Griem,* A.W. Ali, B.H. Ripin, and C.K. Manka** | |
| 13a. TYPE OF REPORT<br>Interim<br>13b. TIME COVERED<br>FROM _____ TO _____ | 14. DATE OF REPORT (Yr., Mo., Day)<br>February 17, 1984<br>15. PAGE COUNT<br>33 |
| 16. SUPPLEMENTARY NOTATION<br>*Present address: University of Maryland, College Park, MD 20742<br>**Present address: Sam Houston State University, Huntsville, TX 77341 (Continues) | |
| 17. COSATI CODES<br>FIELD / GROUP / SUB. GR. | 18. SUBJECT TERMS (Continue on reverse if necessary and identify by block number)<br>Laser-plasma; Shock; Blast wave; Spectroscopy |

19. ABSTRACT (Continue on reverse if necessary and identify by block number)

To simulate HANE phenomena at various altitudes, a pulsed (5 nsec) Nd-laser is focused onto Aℓ or C foil targets surrounded by an ambient gas ($N_2$, $H_2$) at pressures between 15 mTorr and 5 Torr. Temperatures and densities are derived from side-on, time-resolved and time-integrated measurements of absolute spectral line and continuum intensities emitted from the photoionized region ahead of the blast-wave front, and also in the region behind the blast front.

| | |
|---|---|
| 20. DISTRIBUTION/AVAILABILITY OF ABSTRACT<br>UNCLASSIFIED/UNLIMITED ☒ SAME AS RPT ☐ OTIC USERS ☐ | 21. ABSTRACT SECURITY CLASSIFICATION<br>UNCLASSIFIED |
| 22a. NAME OF RESPONSIBLE INDIVIDUAL<br>E. A. McLean | 22b. TELEPHONE NUMBER (Include Area Code)<br>(202) 767-2728<br>22c. OFFICE SYMBOL<br>Code 4700 |

DD FORM 1473, 83 APR EDITION OF 1 JAN 73 IS OBSOLETE.

SECURITY CLASSIFICATION OF THIS PAGE

16. *SUPPLEMENTARY NOTATION* (Continued)

This research was sponsored by the Defense Nuclear Agency under Subtask I25BMXIO, work unit 00024 and work unit title "Early Time High Altitude Nuclear Effects Meeting."

CONTENTS

# SPECTROSCOPIC MEASUREMENTS OF THE LASER-HANE PLASMA

## I. Introduction

One aspect of the laboratory simulation of HANE phenomena using a laser-target interaction is the measurement of the temperature and plasma densities in the photoionized region ahead of the blast-wave front and also at and behind the blast-wave front. Such measurements can then be used to check computer codes written to simulate such an event. Time-integrated and time-resolved spectroscopy is used here to make these measurements, and the results of the first experiment will be given. Spectroscopy has the advantage of being a passive measurement, requiring no physical probes or intense beams which may perturb the plasma during the measurement. Spectroscopy has the disadvantage of not giving complete spatial resolution, unless an Abel inversion procedure is performed, since it integrates along the optical path of the accepted rays. However, we do get some spatial resolution by making our observation at a known distance from the target surface. Data taken in higher pressure regimes, 1.5-5 Torr, will be emphasized in this paper.

## II. Description of Optical Arrangement

The physical layout of our experiment is shown in Fig. 1. The laser beam is incident onto the target from the left, having been focused by an f/6, 1.2-m lens to a focal spot between 250 μm and 1000 μm in diameter. During the course of the experiment, both the laser energy and pulse duration were also varied to produce the desired ion velocities. The target is either a carbon or aluminum foil, typically 4-10 μm thick, and the background gas present in the target chamber is nitrogen, hydrogen, or a mixture of 90% $N_2$ and 10% $H_2$ at pressures ranging from 15 mTorr to 5 Torr. (This corresponds to the range of pressures of HANE events of interest.)

Manuscript approved December 12, 1983.

An optical train to observe the plasma luminosity is set up perpendicular to the laser beam and parallel to the target surface, with the axis of the optical train located 1 cm from the target. In some experiments an aperture is placed between the target surface and the line-of-sight so that the length of the photoionized region can be more accurately measured. (In the experiments described here, this aperture was not used, because observations of both the photoionized plasma and the debris plasma were made, and collisions of the debris with the aperture would have produced undesired spectral intensities.) Most of the measurements were made with the optical train shown in Fig. 1, which consists of a f/2.5, 9-cm f.l. lens, a plane mirror, and a concave mirror. The concave mirror has a 16-inch focal length. This optical train focuses the image of the plasma (magnified 4.25 times) onto the slit of a 1-m spectrograph-monochromator, equipped to take either photographic, time-integrated spectra or else time-resolved spectral data. A RCA-1P28 photomultiplier connected to a fast oscilloscope (Tektronix 7104) gives a system rise time of 3 nsec. The entire optical train including the spectrograph and the photomultipliers is calibrated in situ on an absolute scale using a calibrated tungsten lamp.

## III. Time-Integrated Spectra

Before any time-resolved spectral data were taken, a time-integrated survey was made of the spectra in the wavelength region from 3000 Å to 6500 Å. The spectra were recorded on Polaroid 57 film (ASA 3000) and a suitable exposure could usually be made using one shot of the laser. This data, even though time-integrated, shows which spectral lines are present in

the discharge and gives a rough indication of the relative intensity of the lines.

Figure 2 is a typical spectrum showing the region 3300 Å - 4200 Å. The conditions for this shot are as follows: a laser pulse (120 J, 4.5 nsec) is focused onto an aluminum foil target (4.5 microns thick) in a background of nitrogen gas at a pressure of 165 mTorr. The spectrograph views the plasma located 1 cm from the target surface. A wavelength calibration of the spectrum is made prior to the shot by superimposing the spectrum from a Hg vapor light source. The laser-plasma spectrum shows the molecular bands $N_2$ 3371.3 Å, $N_2$ 3576.9 Å, $N_2^+$ 3884.1 Å, and $N_2^+$ 3914.4 Å; and numerous nitrogen atomic ion lines including NII, NIII, and NIV lines. (Other spectral plates showed NI lines.) Also, the target spectral lines of AlI, AlII and AlIII are clearly seen. From these photographic spectra, one can choose suitable spectral lines for time-resolved observation using a monochromator with photoelectric recording. The data given in the remainder of the report will be taken with photomultiplier recording.

## IV. Time-Resolved Spectral Data

One of the main reasons for taking time-resolved data is that it allows one to separate the photoionized region of the plasma from the plasma region which has been heated by the target debris. Also, photoelectric recording makes it much easier than photographic recording to make absolute intensity measurements of the spectral lines and the continuum.

In the results that are presented here we will be making measurements at three ambient gas pressures, which simulates three different atmospheric altitudes. The three pressures are 15 mTorr of nitrogen, 1.5 Torr of a 90%

nitrogen and 10% hydrogen mixture, and 5 Torr of the 90% $N_2$ and 10% $H_2$ mixture. (The $N_2$,$H_2$ mixture was used because we had hoped to use the profile of one of the hydrogen Balmer lines as a measure of electron density. Due to the low intensity of this line, this technique proved to be impractical, so we used other spectroscopic techniques to determine $N_e$.) It is felt that the small concentration (10%) of hydrogen is going to have little effect on the hydrodynamics or temperatures and densities of the target debris-plasma interaction.

## V. Data Taken at Pressures below 1 Torr ($N_2$,$H_2$)

Three different spectral lines are time-correlated in Figure 3; the molecular ion line $N_2^+$ 3914 Å, the singly-charged nitrogen ion line NII 3995 Å, and the carbon (hydrogen-like) ion CVI 3434 Å. These were obtained under conditions of 15 mTorr $N_2$ ($4.9 \times 10^{14}$ molecules/$cm^3$ or $9.8 \times 10^{14}$ atom/$cm^3$) and a 1.5 mg/$cm^2$ carbon foil target; the bandwidth of the observed signal was 3 Å. As before, for all the runs described here the plane of observation was perpendicular to the laser axis and 1 cm from the target. The laser energy was 8 J in a 3.5-nsec FWHM pulse. The time t=0 corresponds to the time of the peak of the laser pulse. It is readily seen that the $N_2^+$ 3914 Å line intensity rises rapidly from t=0 and then has an apparent second peak at about t=30 nsec. However, the NII 3995 Å line has negligible intensity until about t=23 nsec and then rises rapidly to a peak at about t=30 nsec. The CVI 3434 Å line has a similar rise time behavior to that of the NII 3995 Å line. From these results, we can conclude that the x rays and the UV emitted during the laser-target period can excite and ionize the molecular nitrogen, but do not have sufficient flux to dissociate and further ionize the

higher species of ionization. However, collisions between the target debris, whose time history is clearly indicated by the CVI 3434 Å signal, and the background plasma can easily excite the NII 3995 Å line.

Since we know the time of the peak of the CVI signal and the distance to the point of observation we can determine an average velocity, e.g., $3.3 \times 10^7$ cm/sec, for the conditions shown in Fig. 3. Also, the full-width-half-maximum of the CVI temporal signal of 10 nsec indicates that the debris shell has a thickness of about $(3.3 \times 10^7$ cm/sec) x $(10 \times 10^{-9}$ sec) = 0.33 cm. This is consistent with the shell thickness inferred from dark-field shadowgrams. Another example of these velocity measurements is shown in Fig. 4, where the velocity was measured as a function of the laser energy for hydrogen gas at 15 mTorr pressure. Most of the data were taken with a magnetic field aligned perpendicular to the laser beam, but several of the shots had no magnetic field. The velocity rises quite rapidly with laser energy up to about 10 J on target and then continues to rise but at a much slower rate. There appears to be no dependence of the velocity on the magnetic field. The values of velocity measured using this technique agree favorably with the velocity measurements using time-of-flight charge collectors.

In Fig. 5, the peak intensity of the CVI 3434 Å line is plotted as a function of the incident laser energy. The background gas is hydrogen at a pressure of 15 mTorr. It is noted that the peak line intensity increases linearly with laser energy. However, if the CVI 3434 Å peak line intensity is plotted against pressure of hydrogen for a constant laser energy of 1.5 J as seen in Fig. 6, the line intensity was observed to have a strong minimum in the neighborhood of 5 mTorr pressure. This is may be associated with charge-exchange effects, but needs further work to explain it in detail. There is insufficient data at 15 mTorr to calculate temperatures and densities in the

photoionized and debris regions of the plasma.

## VI. Data Taken at Pressures above 1 Torr (90% $N_2$ + 10% $H_2$)

### A. 1.5-Torr Case.

A time comparison of nitrogen molecular bands with nitrogen atomic and ionic lines at an ambient density of $4.9 \times 10^{16}$ molecules/$cm^3$ ($9.8 \times 10^{16}$ atoms/$cm^3$) is shown in Fig. 7. As before, for all the runs described here the plane of observation was perpendicular to the laser axis and 1 cm from the target and t=0 corresponds to the time of the peak of the laser pulse. The laser energy was ~ 25 J in a 4.5-ns FWHM pulse. The target is an aluminum foil about 2 mm wide and 4.6 μm thick. The $N_2$ 3371 Å band and the $N_2^+$ 3914 Å band have a very similar temporal behavior, i.e., both bands peak at about the same time during the laser pulse with no significant rise at the time the debris passes the point of observation. The NI 4256 Å line, on the other hand, shows a distinct peak during the time of the laser pulse and then a second even larger peak when the debris comes by. The NII 3995 Å only shows a small peak during the laser pulse and a much larger peak when the debris collides with the background plasma, and the NIII 4379 Å shows no intensity until the debris appears. Clearly, under these conditions photoionization alone cannot completely dissociate and ionize the atomic ions.

### B. 5.0-Torr Case.

A similar time comparison of nitrogen molecular bands and atomic and ionic lines for an ambient gas pressure of 5 Torr is shown in Fig. 8. Other conditions are the same as those described in Fig. 7. Although the molecular

bands $N_2$ 3371 Å and $N_2^+$ 3914 Å have a similar sharp rise to that of the 1.5-Torr case, both have a second peak at the time the debris arrives at the point of observation. This second peak was found to be due to the continuum which has a strong peak at that time. The NI 4265 Å line has a very small peak at the time of the laser pulse but a very distinct peak at the time the debris front passes the observed region. Coupled with the distinct peak for the NII 3995 Å line at the time the debris front passes, it would appear that we have a sharp density step as expected from a "snow-plowing" blast wave. (The dark-field shadowgrams have also indicated a similar density step.) The NIII 4379 Å line also has a fairly sharp rise but it peaks about 15 nsec after the peaks of the NI and NII signals.

Also, in this sequence a continuum signal at 4834 Å was recorded. This signal has virtually no intensity during the laser pulse but has an appreciable amplitude when the debris front passes and then decays monotonically. The continuum intensity must be subtracted from the other intensities to get the true intensity of the spectral lines. But a useful benefit of the strong continuum is that we were able to use the absolute continuum intensity to determine the electron density.

In Fig. 9, we show several examples of an intensity step that occurred on the atom, ion and continuum signals just prior to the peak signal, which occurred at the time the blast-wave front passed. This "pre-step" did not occur on every shot, but for the 5 Torr case, it occurred on the majority of the shots. It is interesting to speculate on possible causes for this step. For example, the step could be due to an increase in plasma light emissivity caused by the ultraviolet radiation or fast electrons and ions that are emitted by the expanding shell; it could be caused by a step in density ahead of the debris (seen by J. Stamper in dark-field shadowgrams); or it could be

caused by the proturberances often seen in the blast wavefront under these conditions appearing in the field of view. This phenomena certainly bears further study.

## VII. Analysis of Data

In this section we will discuss the methods we used to calculate the temperatures and densities from the absolute, time-resolved intensity measurements. The equations will be solved by an iterative technique, since we do not have an independent measurement of either the electron density or the electron temperature.

The analysis of the plasma parameters in the photoionized region is based on the intensity from two nitrogen band heads. These are the (0,0) transition from the first negative band system of $N_2^+$ at 3914 Å and the (0,0) transition from the second positive band system of $N_2$ at 3371 Å. From the absolute and the relative intensities of these two bands one obtains the electron density and the electron temperature. The theoretical basis for this analysis and the details of calculations will be published.[1]

The analysis of the data in the debris-background plasma interaction region involved an estimate of the electron temperature, made from observations of the intensities of the lines from the various stages of ionization, and the electron density, made from the absolute measurement of the continuum intensity. The temperature is estimated from the appearance of the highest stage of ionization. Although we saw weak NIV 3479-3483 Å lines in our photographic spectra, Fig. 2, which was taken at a much lower background gas density and a much higher laser energy, we do not expect these lines to have appreciable intensity at 1.5-5 Torr and 25 J laser energy. We

assume that the NIII lines represent the highest stage of ionization present here. This technique of temperature measurement has a large error bracket, so we hope in our next measurements to use other techniques to obtain an electron temperature with a smaller error.

To obtain the electron density from the measurements of the absolute continuum intensities, we have used an equation obtained from Griem,[2] and have made the assumption that the electron density $N_e$, is approximately equal to the ion density, $N_a^z$. since the plasma is predominantly single-ionized. This equation, which includes both recombination radiation and bremsstrahlung contributions, is

$$I = \varepsilon^{z,a} \ell \, \Delta\omega \quad [\text{ergs sec}^{-1}\text{cm}^{-2}\text{sr}^{-1}] \tag{1}$$

where $\varepsilon^{z,a}$ is the emission coefficient in units of energy per unit volume, time, solid angle and angular frequency interval. Since the emission coefficient is a rather long, involved equation (Eq. 5-36, p. 116 of Griem) it is best to get the description of the symbols from Griem.[2]

This equation for the continuum intensity is only weakly dependent on the temperature, so that the large error bracket for the temperature will not change the values for the electron density appreciably.

Two sets of data have been analyzed; one set at an ambient gas pressure of 1.5 Torr and one set at 5 Torr. The data was taken using an aluminum foil target, a background gas mixture of 90% $N_2$ and 10% $H_2$ and a laser energy of 25 J in a 5-nsec pulse. The plane of observation is 1 cm from the target and perpendicular to the laser beam. The optical pathlength, $\ell$, is calculated to be 1.5 cm for the photoionized region and is measured on shadowgrams to be approximately 0.5 cm at the blast-wave front. The results for the 1.5 Torr

measurements are given in Table 1, and the results for the 5.0 Torr measurements are given in Table 2.

Table 1. Table of the measured temperature and densities in the photoionized region and the debris front at an ambient pressure of 1.5 Torr ($4.9 \times 10^{16}$ molecules/$cm^3$).

| | Photoionized Region | Pre-Step (Ahead of Blast Wave) | Blast-Wave Front |
|---|---|---|---|
| Te | 2.5 eV | - | < 14 eV |
| Ne | $3 \times 10^{14} cm^{-3}$ | $5 \times 10^{17} cm^{-3}$ | $9 \times 10^{17} cm^{-3}$ |
| Deg. of Ion | 0.3% | ~ 100% | ~ 100% |
| Density step | - | - | 10 |

Assuming $Ne \simeq N^+$

Table 2. Table of the measured temperature and densities in the photoionized region and the debris front at an ambient pressure of 5 Torr ($1.6 \times 10^{17}$ molecules/$cm^3$).

| | Photoionized Region | Pre-Step (Ahead of Blast Wave) | Blast-Wave Front |
|---|---|---|---|
| Te | 1.85 eV | - | < 14 eV |
| Ne | $6 \times 10^{14} cm^{-3}$ | $2 \times 10^{18} cm^{-3}$ | $5 \times 10^{18} cm^{-3}$ |
| Deg. of Ion | 0.2% | ~ 100% | ~ 100% |
| Density Step | - | - | 15 |

Assuming $Ne \simeq N^+$

In addition to the spectroscopic measurement of the electron density at the debris front at 5 Torr ambient pressure, an estimate of the minimum jump in $N_e$ can be obtained from analysis of the dark field shadowgrams. Such an estimate gave $N_e > 1 \times 10^{17}$ $cm^{-3}$. Although this is over an order-of-magnitude

lower than the spectroscopic measurement of $N_e$, it is a minimum value. The spectroscopic measurement of $N_e$ is felt to be the more accurate measurement of electron density.

Since the density of the ions in the blast-wave front for the 5 Torr case is about $5 \times 10^{18}$ $cm^{-3}$, which is about 15 times the ambient density of the nitrogen atoms, it is necessary to have a snow plowing of ions into a shell of similar ion density. This is consistent with the dark field shadowgrams which show a definite shell structure, and also with the analysis of the velocity of the shell as that due to a blast wave. For the 1.5 Torr case, the density of the ions is about $9 \times 10^{17} cm^{-3}$ in the blast-wave front, which is about 10 times the background atom density. (This latter density step is about the same as that calculated using a blast-wave model.[3,4]

## VIII. Summary

The spectroscopic data presented in this report is our first attempt to measure absolute intensities of spectral lines and continuum in this experiment and then carry out the analysis of the data. In the process, we have established approximate values for the plasma temperature and densities. More accurate values will be obtained during our next experimental series.

The time-resolved spectral data allows the separation of the photoionized region from the region excited and ionized by the debris. In the 1.5-5 Torr pressure range, a density step was seen ahead of the main peak in the signal. The interpretation of this density step has not been established at this time and warrrants further study.

## IX. Acknowledgments

This work was supported by the Defense Nuclear Agency. The authors would like to acknowledge useful discussions with S.P. Obenschain, J. Grun, M.J. Herbst, R.R. Whitlock, and F. Young of NRL, and R. Kilb of MRC. The technical assistance of N. Nocerino, E. Turbyfill, M. Fink and B. Sands is greatly appreciated.

## References

1. A.W. Ali, "The Electron Density and Temperature in the Photoionized Background Gas ($N_2$) Surrounding a Laser Produced Plasma," Naval Research Laboratory Memorandum Report (in press).

2. Hans R. Griem, "Plasma Spectroscopy," (McGraw-Hill, New York, 1964).

3. Ya.B. Zel'dovich and Yu. P. Raizer, "Physics of Shock Waves and High-Temperature Hydrodynamic Phenomena," Edited by Wallace D. Hayes and Ronald F. Probstein (Academic Press, New York, 1966), Vol. 1.

4. B.H. Ripin, J.A. Stamper, and E.A. McLean, "Blast-Wave Analysis of High-Pressure Shells," Naval Research Laboratory Memorandum Report (in press).

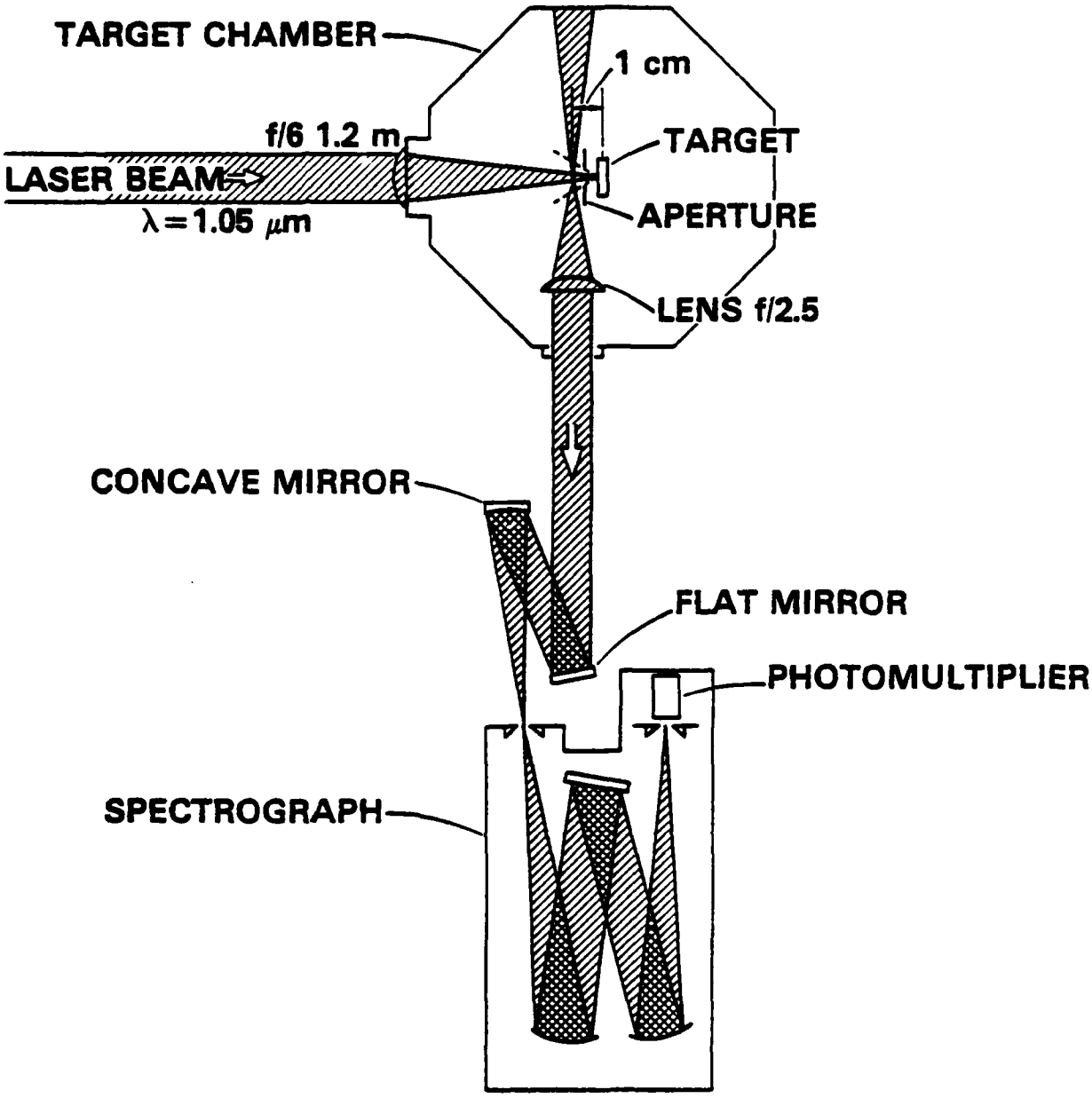


**Figure 1**

Experimental arrangement.

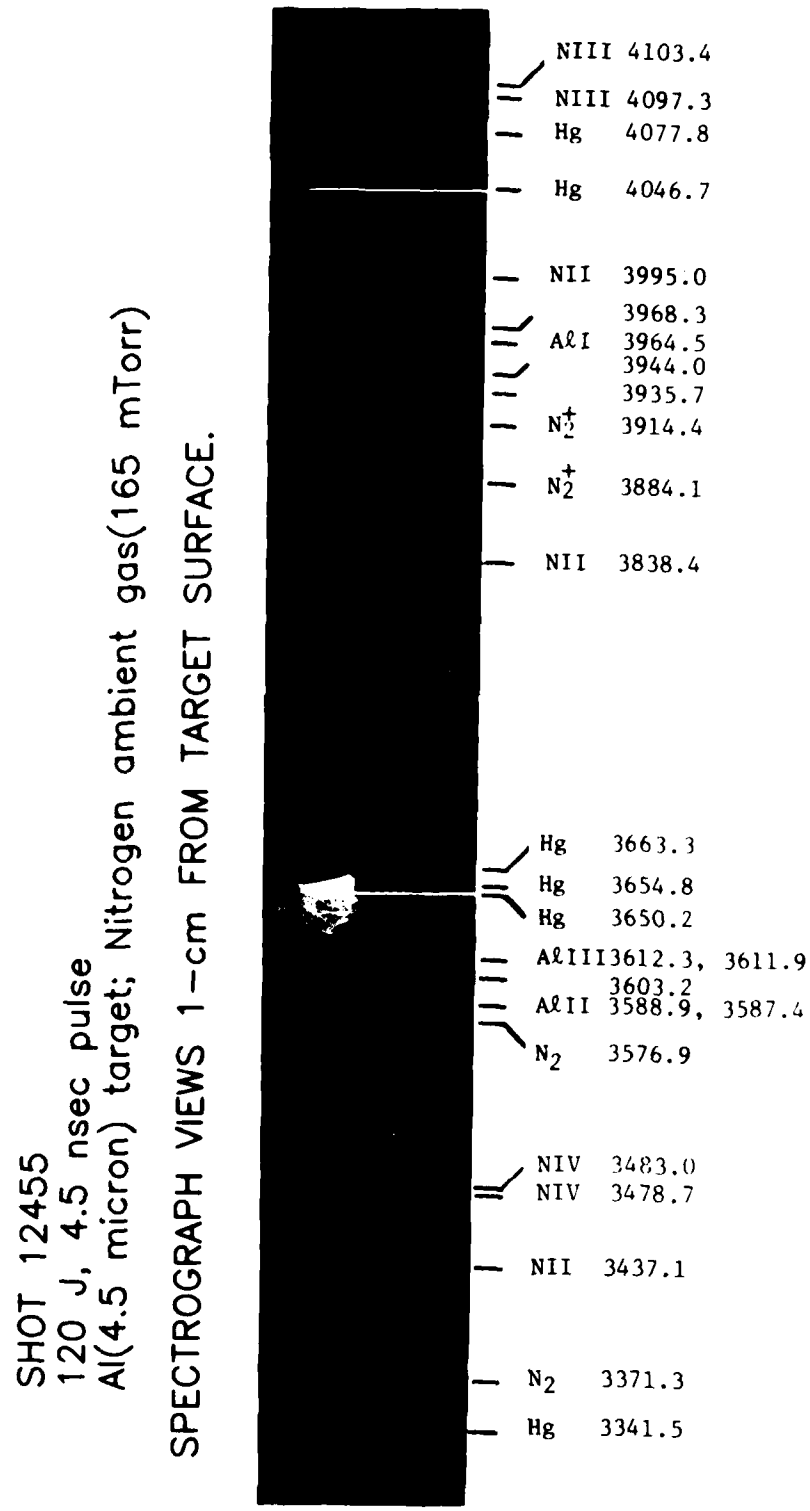


Figure 2

Typical photographic spectrum for conditions shown on figure. The mercury (Hg) lines are superimposed on the spectrum prior to the shot to give a wavelength calibration. The spectral line identifications are given next to the lines.

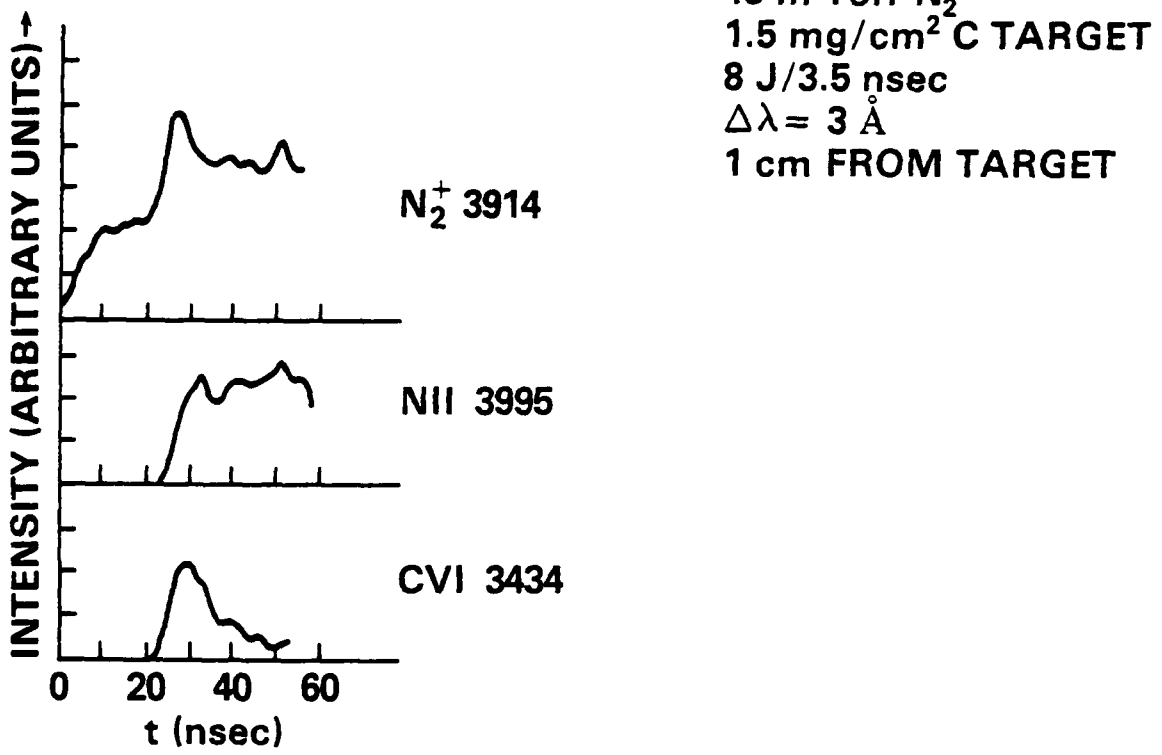


Figure 3

A temporal comparison of the spectral line intensities for the background gas pressure of 15 mTorr. (Other conditions are given on the figure.) The t=0 time is the time of the peak of the laser pulse. The ordinate scale is in arbitrary units and the zero intensity level is the value before t=0 time.

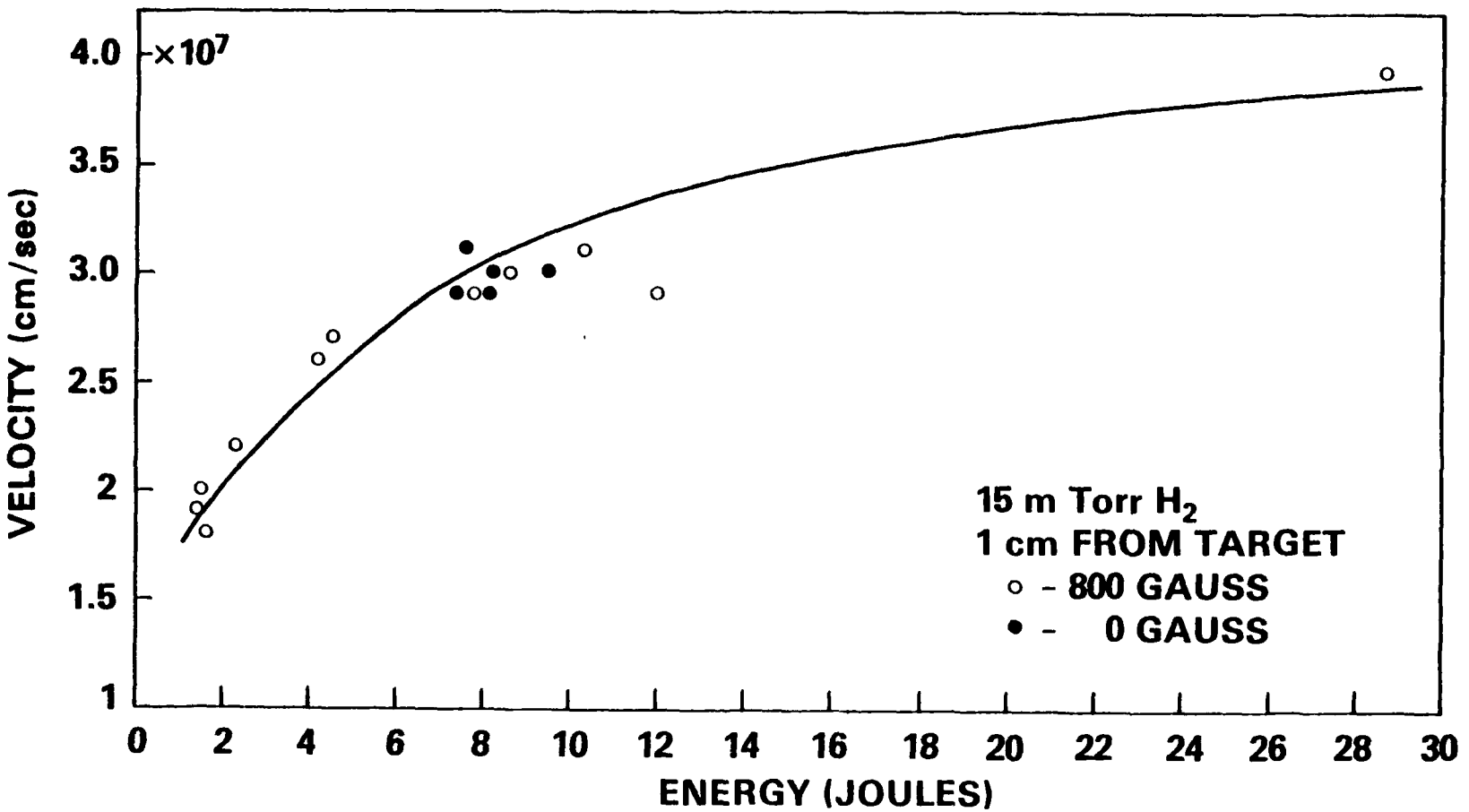


Figure 4

Average velocity of the debris front from the time-of-flight of the $C^{5+}$ (CVI) ions versus laser energy. Presence of the magnetic field did not modify velocity of $C^{5+}$ ions.

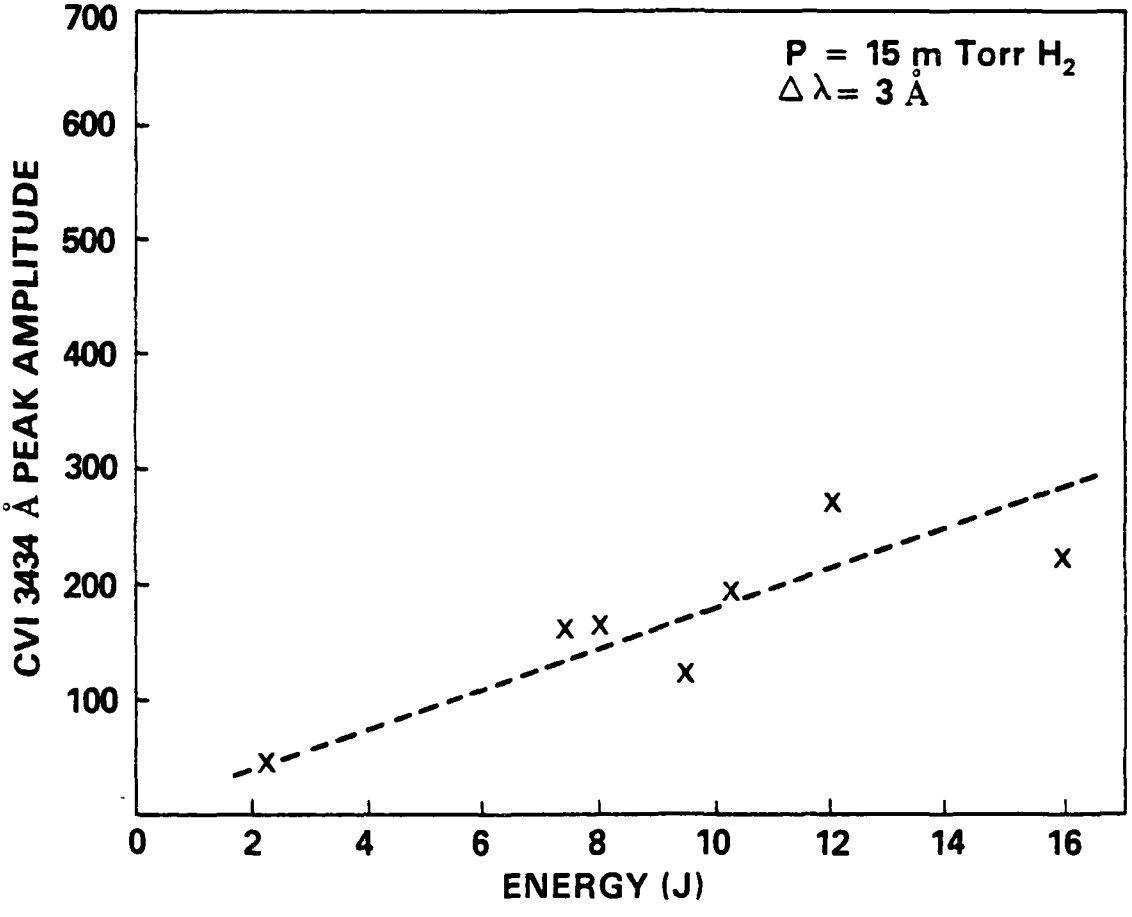


Figure 5

Peak CVI 3434 Å line intensity versus laser energy at constant pressure (15 mTorr $H_2$).

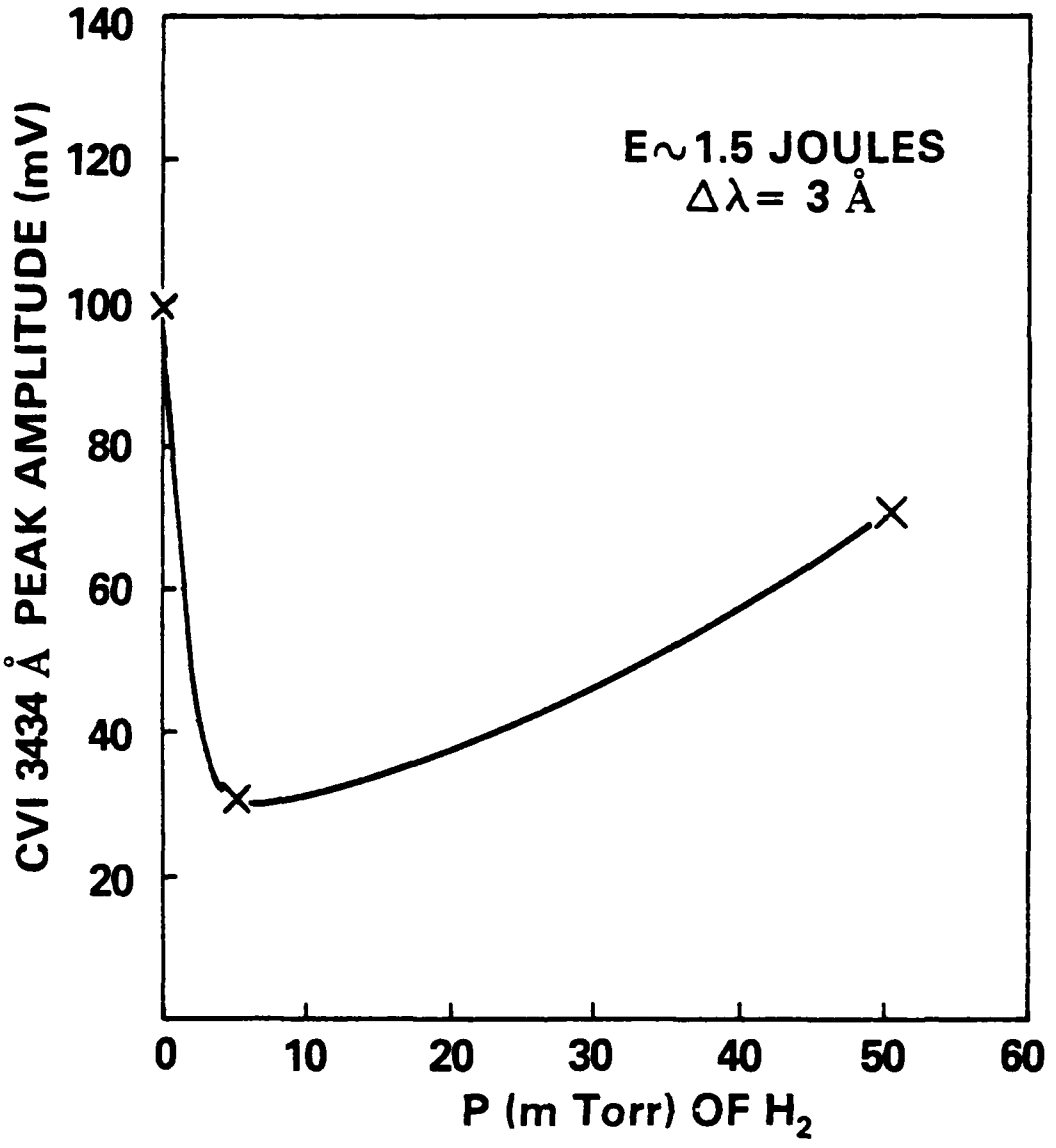


Figure 6

Peak CVI 3434 Å line intensity versus background gas pressure at constant laser energy (1.5 Joules).

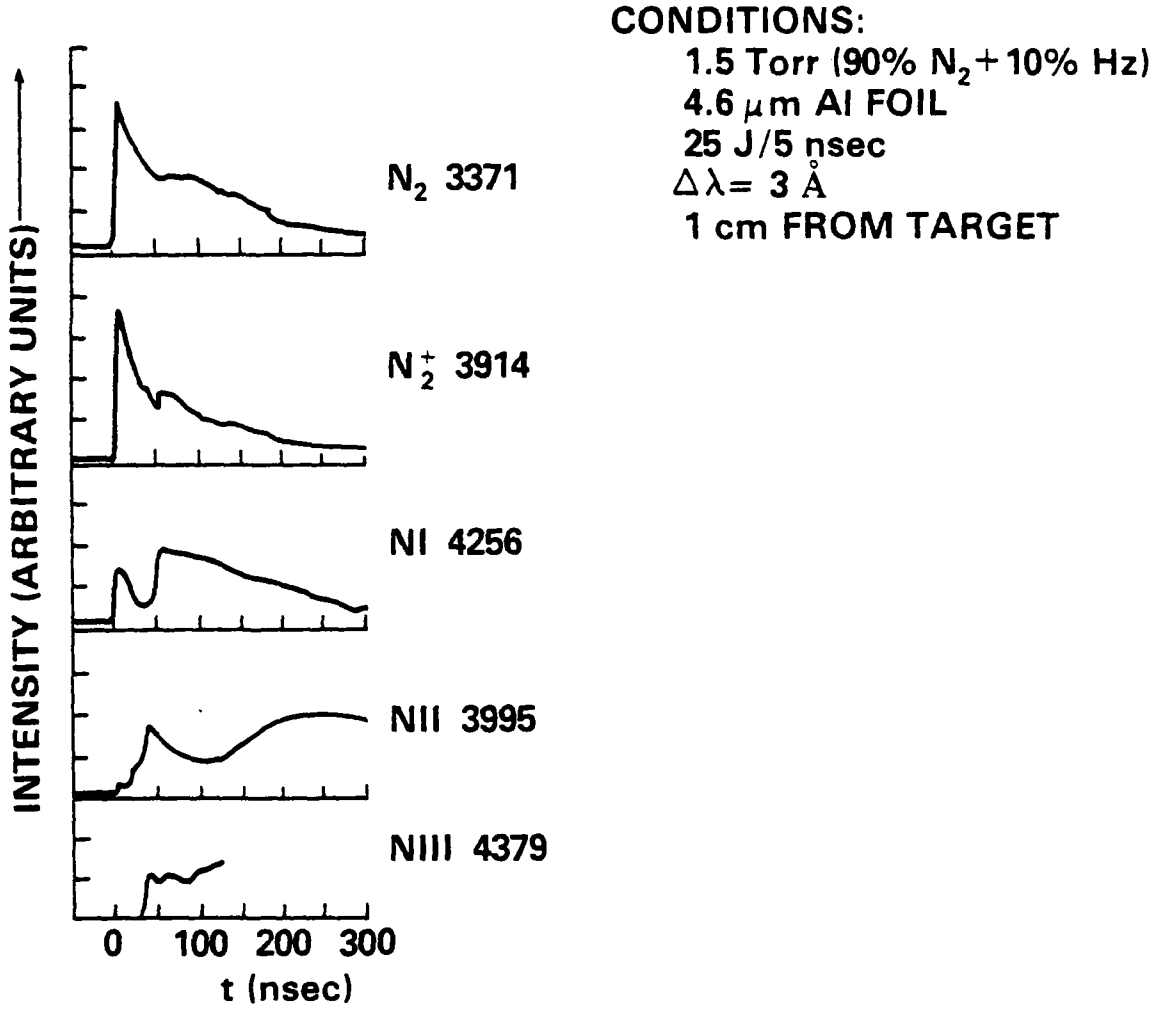


Figure 7

A temporal comparison of the spectral line intensities for the background gas pressure of 1.5 Torr. (Other conditions are given on the figure.) The t=0 time is the time of the peak of the laser pulse. The line intensity is zero before t=0 time.

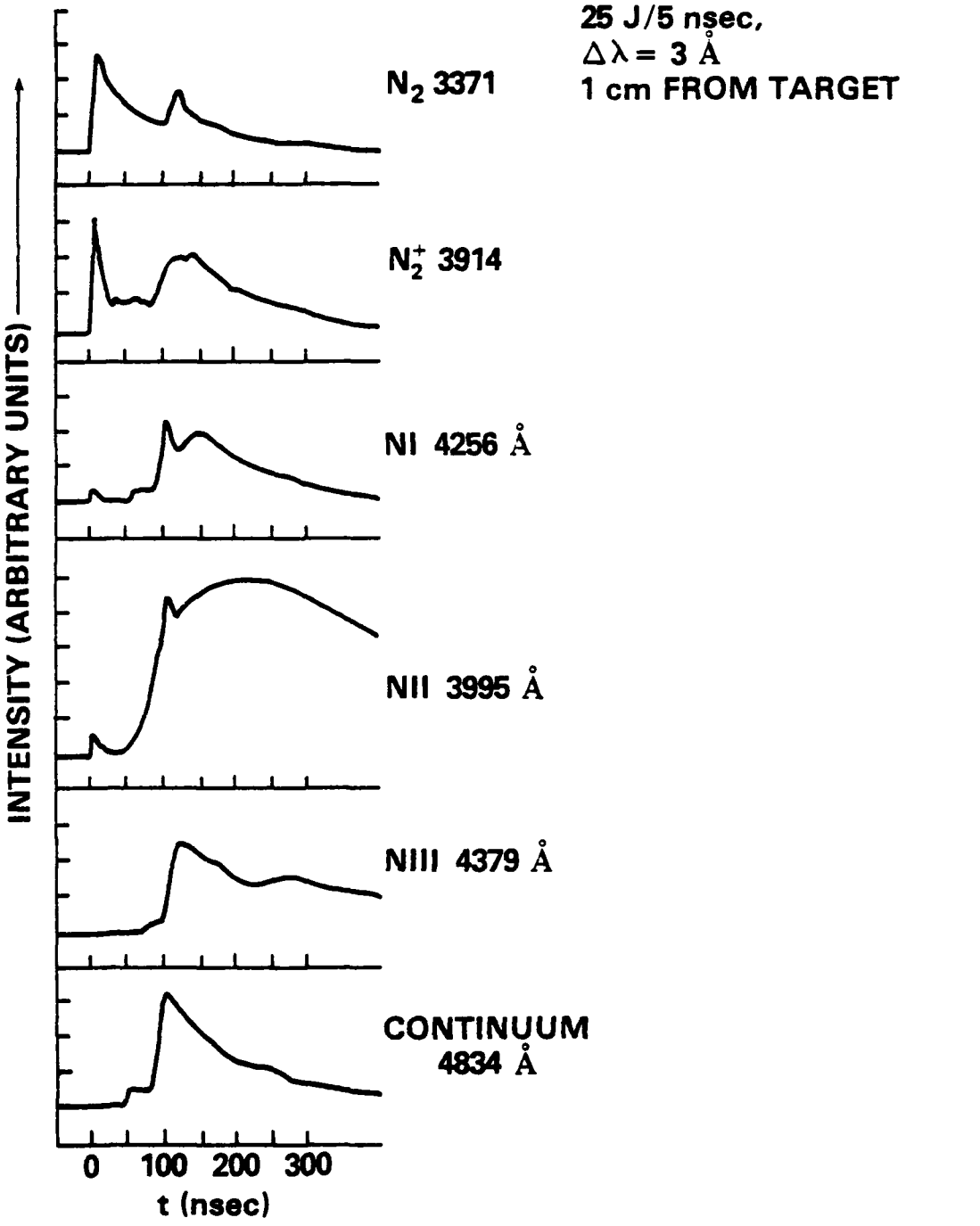


Figure 8

A temporal comparison of the spectral line and continuum intensities for a background gas pressure of 5.0 Torr. Other conditions are given on figure. The t=0 time is the time of the laser peak.

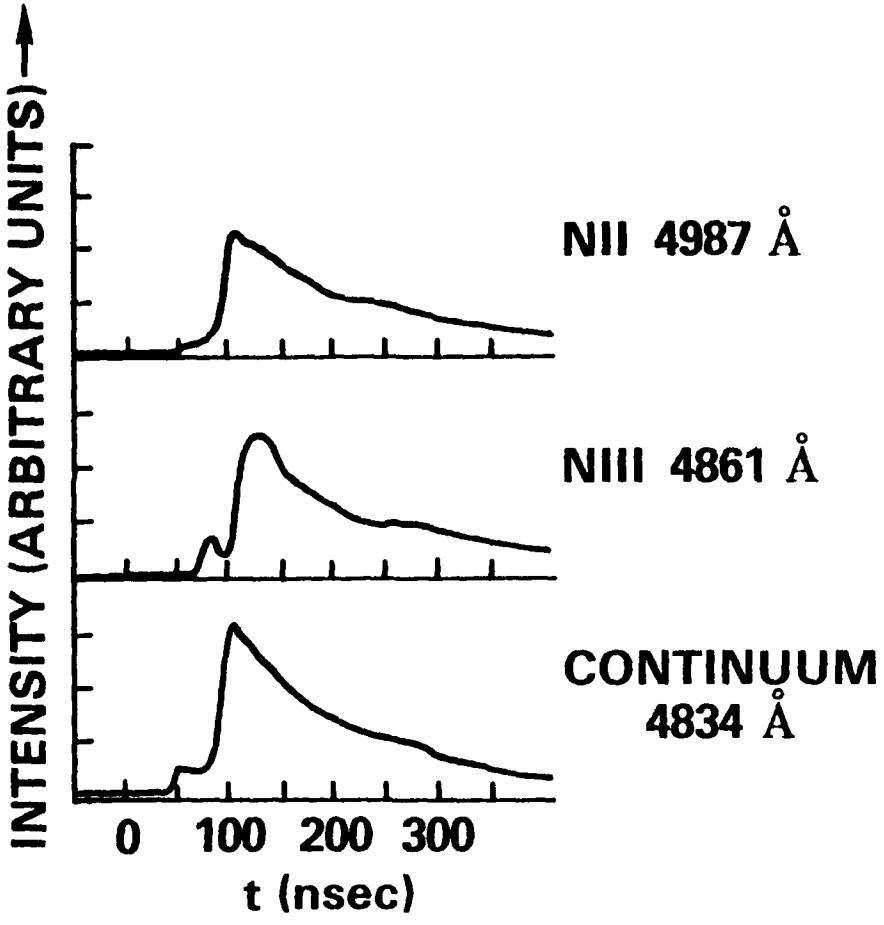


**CONDITIONS:**

- 5 Torr (90% $N_2$ + 10% Hz)
- 4.6 $\mu$m Al FOIL
- 25 J/5 nsec
- $\Delta\lambda = 3$ Å
- 1 cm FROM TARGET

Figure 9

Sample intensity-time traces showing a pre-step ahead of the debris for the case of a background pressure of 5 Torr. Conditions are shown on figure.

# DISTRIBUTION LIST

DEPARTMENT OF DEFENSE

ASSISTANT SECRETARY OF DEFENSE
COMM, CMD, CONT 7 INTELL
WASHINGTON, D.C. 20301

DIRECTOR
COMMAND CONTROL TECHNICAL CENTER
PENTAGON RM BE 685
WASHINGTON, D.C. 20301
01CY ATTN C-650
01CY ATTN C-312 R. MASON

DIRECTOR
DEFENSE ADVANCED RSCH PROJ AGENCY
ARCHITECT BUILDING
1400 WILSON BLVD.
ARLINGTON, VA. 22209
01CY ATTN NUCLEAR MONITORING RESEARCH
01CY ATTN STRATEGIC TECH OFFICE

DEFENSE COMMUNICATION ENGINEER CENTER
1860 WIEHLE AVENUE
RESTON, VA. 22090
01CY ATTN CODE R410
01CY ATTN CODE R812

DEFENSE TECHNICAL INFORMATION CENTER
CAMERON STATION
ALEXANDRIA, VA. 22314
02CY

DIRECTOR
DEFENSE NUCLEAR AGENCY
WASHINGTON, D.C. 20305
01CY ATTN STVL
04CY ATTN TITL
01CY ATTN DDST
03CY ATTN RAAE

COMMANDER
FIELD COMMAND
DEFENSE NUCLEAR AGENCY
KIRTLAND, AFB, NM 87115
01CY ATTN FCPR

DEFENSE NUCLEAR AGENCY
SAO/DNA
BUILDING 20676
KIRTLAND AFB, NM 87115
01CY D.C. THORNBURG

DIRECTOR
INTERSERVICE NUCLEAR WEAPONS SCHOOL
KIRTLAND AFB, NM 87115
01CY ATTN DOCUMENT CONTROL

JOINT CHIEFS OF STAFF
WASHINGTON, D.C. 20301
01CY ATTN J-3 WWMCCS EVALUATION OFFICE

DIRECTOR
JOINT STRAT TGT PLANNING STAFF
OFFUTT AFB
OMAHA, NB 68113
01CY ATTN JLTW-2
01CY ATTN JPST G. GOETZ

CHIEF
LIVERMORE DIVISION FLD COMMAND DNA
DEPARTMENT OF DEFENSE
LAWRENCE LIVERMORE LABORATORY
P.O. BOX 808
LIVERMORE, CA 94550
01CY ATTN FCPRL

COMMANDANT
NATO SCHOOL (SHAPE)
APO NEW YORK 09172
01CY ATTN U.S. DOCUMENTS OFFICER

UNDER SECY OF DEF FOR RSCH & ENGRG
DEPARTMENT OF DEFENSE
WASHINGTON, D.C. 20301
01CY ATTN STRATEGIC & SPACE SYSTEMS (OS)

WWMCCS SYSTEM ENGINEERING ORG
WASHINGTON, D.C. 20305
01CY ATTN R. CRAWFORD

COMMANDER/DIRECTOR
ATMOSPHERIC SCIENCES LABORATORY
U.S. ARMY ELECTRONICS COMMAND
WHITE SANDS MISSILE RANGE, NM 88002
01CY ATTN DELAS-EO F. NILES

DIRECTOR
BMD ADVANCED TECH CTR
HUNTSVILLE OFFICE
P.O. BOX 1500
HUNTSVILLE, AL 35807
01CY ATTN ATC-T MELVIN T. CAPPS
01CY ATTN ATC-O W. DAVIES
01CY ATTN ATC-R DON RUSS

PROGRAM MANAGER
BMD PROGRAM OFFICE
5001 EISENHOWER AVENUE
ALEXANDRIA, VA 22333
01CY ATTN DACS-BMT J. SHEA

CHIEF C-E- SERVICES DIVISION
U.S. ARMY COMMUNICATIONS CMD
PENTAGON RM 18269
WASHINGTON, D.C. 20310
01CY ATTN C- E-SERVICES DIVISION

COMMANDER
FRADCOM TECHNICAL SUPPORT ACTIVITY
DEPARTMENT OF THE ARMY
FORT MONMOUTH, N.J. 07703
01CY ATTN DRSEL-NL-RD H. BENNET
01CY ATTN DRSEL-PL-ENV H. BOMKE
01CY ATTN J.E. QUIGLEY

COMMANDER
U.S. ARMY COMM-ELEC ENGRG INSTAL AGY
FT. HUACHUCA, AZ 85613
01CY ATTN CCC-EMEO GEORGE LANE

COMMANDER
U.S. ARMY FOREIGN SCIENCE & TECH CTR
220 7TH STREET, NE
CHARLOTTESVILLE, VA 22901
01CY ATTN DRXST-SD

COMMANDER
U.S. ARMY MATERIAL DEV & READINESS CMD
5001 EISENHOWER AVENUE
ALEXANDRIA, VA 22333
01CY ATTN DRCLDC J.A. BENDER

COMMANDER
U.S. ARMY NUCLEAR AND CHEMICAL AGENCY
7500 BACKLICK ROAD
BLDG 2073
SPRINGFIELD, VA 22150
01CY ATTN LIBRARY

DIRECTOR
U.S. ARMY BALLISTIC RESEARCH LABORATORY
ABERDEEN PROVING GROUND, MD 21005
01CY ATTN TECH LIBRARY EDWARD BAICY

COMMANDER
U.S. ARMY SATCOM AGENCY
FT. MONMOUTH, NJ 07703
01CY ATTN DOCUMENT CONTROL

COMMANDER
U.S. ARMY MISSILE INTELLIGENCE AGENCY
REDSTONE ARSENAL, AL 35809
01CY ATTN JIM GAMBLE

DIRECTOR
U.S. ARMY TRADOC SYSTEMS ANALYSIS ACTIVITY
WHITE SANDS MISSILE RANGE, NM 88002
01CY ATTN ATAA-SA
01CY ATTN TCC/F. PAYAN JR.
01CY ATTN ATTA-TAC LTC J. HESSE

COMMANDER
NAVAL ELECTRONIC SYSTEMS COMMAND
WASHINGTON, D.C. 20360
01CY ATTN NAVALEX 034 T. HUGHES
01CY ATTN PME 117
01CY ATTN PME 117-T
01CY ATTN CODE 3011

COMMANDING OFFICER
NAVAL INTELLIGENCE SUPPORT CTR
4301 SUITLAND ROAD, BLDG. 5
WASHINGTON, D.C. 20390
01CY ATTN MR. DUBBIN STIC 12
01CY ATTN NISC-50
01CY ATTN CODE 5404 J. GALET

COMMANDER
NAVAL OCEAN SYSTEMS CENTER
SAN DIEGO, CA 92152
01CY ATTN J. FERGUSON

NAVAL RESEARCH LABORATORY
WASHINGTON, D.C. 20375
01CY ATTN CODE 4700 S. L. Ossakow
26 CYS IF UNCLASS. 1 CY IF CLASS)
01CY ATTN CODE 4701 I Vitkovitsky
01CY ATTN CODE 4780 J. Huba (10
CYS IF UNCLASS, 1 CY IF CLASS)
01CY ATTN CODE 7500
01CY ATTN CODE 7550
01CY ATTN CODE 7580
01CY ATTN CODE 7551
01CY ATTN CODE 7555
01CY ATTN CODE 4730 E. MCLEAN
01CY ATTN CODE 4108
01CY ATTN CODE 4730 B. RIPIN
20CY ATTN CODE 2628
100CY ATTN CODE 4730

COMMANDER
NAVAL SEA SYSTEMS COMMAND
WASHINGTON, D.C. 20362
01CY ATTN CAPT R. PITKIN

COMMANDER
NAVAL SPACE SURVEILLANCE SYSTEM
DAHLGREN, VA 22448
01CY ATTN CAPT J.H. BURTON

OFFICER-IN-CHARGE
NAVAL SURFACE WEAPONS CENTER
WHITE OAK, SILVER SPRING, MD 20910
01CY ATTN CODE F31

DIRECTOR
STRATEGIC SYSTEMS PROJECT OFFICE
DEPARTMENT OF THE NAVY
WASHINGTON, D.C. 20376
01CY ATTN NSP-2141
01CY ATTN NSSP-2722 FRED WIMBERLY

COMMANDER
NAVAL SURFACE WEAPONS CENTER
DAHLGREN LABORATORY
DAHLGREN, VA 22448
01CY ATTN CODE DF-14 R. BUTLER

OFFICER OF NAVAL RESEARCH
ARLINGTON, VA 22217
01CY ATTN CODE 465
01CY ATTN CODE 461
01CY ATTN CODE 402
01CY ATTN CODE 420
01CY ATTN CODE 421

COMMANDER
AEROSPACE DEFENSE COMMAND/DC
DEPARTMENT OF THE AIR FORCE
ENT AFB, CO 80912
01CY ATTN DC MR. LONG

COMMANDER
AEROSPACE DEFENSE COMMAND/XPD
DEPARTMENT OF THE AIR FORCE
ENT AFB, CO 80912
01CY ATTN XPDQQ
01CY ATTN XP

AIR FORCE GEOPHYSICS LABORATORY
HANSCOM AFB, MA 01731
01CY ATTN OPR HAROLD GARDNER
01CY ATTN LKB KENNETH S.W. CHAMPION
01CY ATTN OPR ALVA T. STAIR
01CY ATTN PHD JURGEN BUCHAU
01CY ATTN PHD JOHN P. MULLEN

AF WEAPONS LABORATORY
KIRTLAND AFT, NM 87117
01CY ATTN SUL
01CY ATTN CA ARTHUR H. GUENTHER
01CY ATTN NTYCE 1LT. G. KRAJEI

AFTAC
PATRICK AFB, FL 32925
01CY ATTN TF/MAJ WILEY
01CY ATTN TN

AIR FORCE AVIONICS LABORATORY
WRIGHT-PATTERSON AFB, OH 45433
01CY ATTN AAD WADE HUNT
01CY ATTN AAD ALLEN JOHNSON

DEPUTY CHIEF OF STAFF
RESEARCH, DEVELOPMENT, & ACQ
DEPARTMENT OF THE AIR FORCE
WASHINGTON, D.C. 20330
01CY ATTN AFRDQ

HEADQUARTERS
ELECTRONIC SYSTEMS DIVISION
DEPARTMENT OF THE AIR FORCE
HANSCOM AFB, MA 01731
01CY ATTN J. DEAS

HEADQUARTERS
ELECTRONIC SYSTEMS DIVISION/YSEA
DEPARTMENT OF THE AIR FORCE
HANSCOM AFB, MA 01732
01CY ATTN YSEA

HEADQUARTERS
ELECTRONIC SYSTEMS DIVISION/DC
DEPARTMENT OF THE AIR FORCE
HANSCOM AFB, MA 01731
01CY ATTN DCKC MAJ J.C. CLARK

COMMANDER
FOREIGN TECHNOLOGY DIVISION, AFSC
WRIGHT-PATTERSON AFB, OH 45433
01CY ATTN NICD LIBRARY
01CY ATTN ETDP B. BALLARD

COMMANDER
ROME AIR DEVELOPMENT CENTER, AFSC
GRIFFISS AFB, NY 13441
01CY ATTN DOC LIBRARY/TSLD
01CY ATTN OCSE V. COYNE

SAMSO/SZ
POST OFFICE BOX 92960
WORLDWAY POSTAL CENTER
LOS ANGELES, CA 90009
(SPACE DEFENSE SYSTEMS)
01CY ATTN SZJ

STRATEGIC AIR COMMAND/XPFS
OFFUTT AFB, NB 68113
01CY ATTN ADWATE MAJ BRUCE BAUER
01CY ATTN NRT
01CY ATTN DOK CHIEF SCIENTIST

SAMSO/SK
P.O. BOX 92960
WORLDWAY POSTAL CENTER
LOS ANGELES, CA 90009
01CY ATTN SKA (SPACE COMM SYSTEMS)
M. CLAVIN

SAMSO/MN
NORTON AFB, CA 92409
(MINUTEMAN)
01CY ATTN MNNL

COMMANDER
ROME AIR DEVELOPMENT CENTER, AFSC
HANSCOM AFB, MA 01731
01CY ATTN EEP A. LORENTZEN

DEPARTMENT OF ENERGY
LIBRARY ROOM G-042
WASHINGTON, D.C. 20545
01CY ATTN DOC CON FOR A. LABOWITZ

DEPARTMENT OF ENERGY
ALBUQUERQUE OPERATIONS OFFICE
P.O. BOX 5400
ALBUQUERQUE, NM 87115
01CY ATTN DOC CON FOR D. SHERWOOD

EG&G, INC.
LOS ALAMOS DIVISION
P.O. BOX 809
LOS ALAMOS, NM 85544
01CY ATTN DOC CON FOR J. BREEDLOVE

UNIVERSITY OF CALIFORNIA
LAWRENCE LIVERMORE LABORATORY
P.O. BOX 808
LIVERMORE, CA 94550
01CY ATTN DOC CON FOR TECH INFO DEPT
01CY ATTN DOC CON FOR L-389 R. OTT
01CY ATTN DOC CON FOR L-31 R. HAGER
01CY ATTN DOC CON FOR L-46 F. SEWARD

LOS ALAMOS NATIONAL LABORATORY
P.O. BOX 1663
LOS ALAMOS, NM 87545
01CY ATTN DOC CON FOR J. WOLCOTT
01CY ATTN DOC CON FOR R.F. TASCHEK
01CY ATTN DOC CON FOR E. JONES
01CY ATTN DOC CON FOR J. MALIK
01CY ATTN DOC CON FOR R. JEFFRIES
01CY ATTN DOC CON FOR J. ZINN
01CY ATTN DOC CON FOR P. KEATON
01CY ATTN DOC CON FOR D. WESTERVELT
01CY ATTN D. SAPPENFIELD

SANDIA LABORATORIES
P.O. BOX 5800
ALBUQUERQUE, NM 87115
01CY ATTN DOC CON FOR W. BROWN
01CY ATTN DOC CON FOR A. THORNBROUGH
01CY ATTN DOC CON FOR T. WRIGHT
01CY ATTN DOC CON FOR D. DAHLGREN
01CY ATTN DOC CON FOR 3141
01CY ATTN DOC CON FOR SPACE PROJECT DIV

SANDIA LABORATORIES
LIVERMORE LABORATORY
P.O. BOX 969
LIVERMORE, CA 94550
01CY ATTN DOC CON FOR B. MURPHEY
01CY ATTN DOC CON FOR T. COOK

OFFICE OF MILITARY APPLICATION
DEPARTMENT OF ENERGY
WASHINGTON, D.C. 20545
01CY ATTN DOC CON DR. YO SONG

OTHER GOVERNMENT

DEPARTMENT OF COMMERCE
NATIONAL BUREAU OF STANDARDS
WASHINGTON, D.C. 20234
01CY (ALL CORRES: ATTN SEC OFFICER FOR)

INSTITUTE FOR TELECOM SCIENCES
NATIONAL TELECOMMUNICATIONS & INFO ADMIN
BOULDER, CO 80303
01CY ATTN A. JEAN (UNCLASS ONLY)
01CY ATTN W. UTLAUT
01CY ATTN D. CROMBIE
01CY ATTN L. BERRY

NATIONAL OCEANIC & ATMOSPHERIC ADMIN
ENVIRONMENTAL RESEARCH LABORATORIES
DEPARTMENT OF COMMERCE
BOULDER, CO 80302
01CY ATTN R. GRUBB
01CY ATTN AERONOMY LAB G. REID

DEPARTMENT OF DEFENSE CONTRACTORS

AEROSPACE CORPORATION
P.O. BOX 92957
LOS ANGELES, CA 90009
01CY ATTN I. GARFUNKEL
01CY ATTN T. SALMI
01CY ATTN V. JOSEPHSON
01CY ATTN S. BOWER
01CY ATTN D. OLSEN

ANALYTICAL SYSTEMS ENGINEERING CORP
5 OLD CONCORD ROAD
BURLINGTON, MA 01803
01CY ATTN RADIO SCIENCES

AUSTIN RESEARCH ASSOC., INC.
1901 RUTLAND DRIVE
AUSTIN, TX 78758
01CY ATTN L. SLOAN
01CY ATTN R. THOMPSON

BERKELEY RESEARCH ASSOCIATES, INC.
P.O. BOX 983
BERKELEY, CA 94701
01CY ATTN J. WORKMAN
01CY ATTN C. PRETTIE
01CY ATTN S. BRECHT

BOEING COMPANY, THE
P.O. BOX 3707
SEATTLE, WA 98124
01CY ATTN G. KEISTER
01CY ATTN D. MURRAY
01CY ATTN G. HALL
01CY ATTN J. KENNEY

CHARLES STARK DRAPER LABORATORY, INC.
555 TECHNOLOGY SQUARE
CAMBRIDGE, MA 02139
01CY ATTN D.B. COX
01CY ATTN J.P. GILMORE

COMSAT LABORATORIES
LINTHICUM ROAD
CLARKSBURG, MD 20734
01CY ATTN G. HYDE

CORNELL UNIVERSITY
DEPARTMENT OF ELECTRICAL ENGINEERING
ITHACA, NY 14850
01CY ATTN D.T. FARLEY, JR.

ELECTROSPACE SYSTEMS, INC.
BOX 1359
RICHARDSON, TX 75080
01CY ATTN H. LOGSTON
01CY ATTN SECURITY (PAUL PHILLIPS)

EOS TECHNOLOGIES, INC.
606 Wilshire Blvd.
Santa Monica, Calif 90401
01CY ATTN C.B. GABBARD

ESL, INC.
495 JAVA DRIVE
SUNNYVALE, CA 94086
01CY ATTN J. ROBERTS
01CY ATTN JAMES MARSHALL

GENERAL ELECTRIC COMPANY
SPACE DIVISION
VALLEY FORGE SPACE CENTER
GODDARD BLVD KING OF PRUSSIA
P.O. BOX 8555
PHILADELPHIA, PA 19101
01CY ATTN M.H. BORTNER SPACE SCI LAB

GENERAL ELECTRIC COMPANY
P.O. BOX 1122
SYRACUSE, NY 13201
01CY ATTN F. REIBERT

GENERAL ELECTRIC TECH SERVICES CO., INC.
HMES
COURT STREET
SYRACUSE, NY 13201
  01CY ATTN G. MILLMAN

GEOPHYSICAL INSTITUTE
UNIVERSITY OF ALASKA
FAIRBANKS, AK 99701
  (ALL CLASS ATTN: SECURITY OFFICER)
  01CY ATTN T.N. DAVIS (UNCLASS ONLY)
  01CY ATTN TECHNICAL LIBRARY
  01CY ATTN NEAL BROWN (UNCLASS ONLY)

GTE SYLVANIA, INC.
ELECTRONICS SYSTEMS GRP-EASTERN DIV
77 A STREET
NEEDHAM, MA 02194
  01CY ATTN DICK STEINHOF

HSS, INC.
2 ALFRED CIRCLE
BEDFORD, MA 01730
  01CY ATTN DONALD HANSEN

ILLINOIS, UNIVERSITY OF
107 COBLE HALL
150 DAVENPORT HOUSE
CHAMPAIGN, IL 61820
  (ALL CORRES ATTN DAN MCCLELLAND)
  01CY ATTN K. YEH

INSTITUTE FOR DEFENSE ANALYSES
1801 NO. BEAUREGARD STREET
ALEXANDRIA, VA 22311
  01CY ATTN J.M. AEIN
  01CY ATTN ERNEST BAUER
  01CY ATTN HANS WOLFARD
  01CY ATTN JOEL BENGSTON

INTL TEL & TELEGRAPH CORPORATION
500 WASHINGTON AVENUE
NUTLEY, NJ 07110
  01CY ATTN TECHNICAL LIBRARY

JAYCOR
11011 TORREYANA ROAD
P.O. BOX 85154
SAN DIEGO, CA 92138
  01CY ATTN J.L. SPERLING

JOHNS HOPKINS UNIVERSITY
APPLIED PHYSICS LABORATORY
JOHNS HOPKINS ROAD
LAUREL, MD 20810
  01CY ATTN DOCUMENT LIBRARIAN
  01CY ATTN THOMAS POTEMRA
  01CY ATTN JOHN DASSOULAS

KAMAN SCIENCES CORP
P.O. BOX 7463
COLORADO SPRINGS, CO 80933
  01CY ATTN T. MEAGHER

KAMAN TEMPO-CENTER FOR ADVANCED STUDIES
816 STATE STREET (P.O DRAWER QQ)
SANTA BARBARA, CA 93102
  01CY ATTN DASIAC
  01CY ATTN WARREN S. KNAPP
  01CY ATTN WILLIAM MCNAMARA
  01CY ATTN B. GAMBILL

LINKABIT CORP
10453 ROSELLE
SAN DIEGO, CA 92121
  01CY ATTN IRWIN JACOBS

LOCKHEED MISSILES & SPACE CO., INC
P.O. BOX 504
SUNNYVALE, CA 94088
  01CY ATTN DEPT 60-12
  01CY ATTN D.R. CHURCHILL

LOCKHEED MISSILES & SPACE CO., INC.
3251 HANOVER STREET
PALO ALTO, CA 94304
  01CY ATTN MARTIN WALT DEPT 52-12
  01CY ATTN W.L. IMHOF DEPT 52-12
  01CY ATTN RICHARD G. JOHNSON DEPT 52-12
  01CY ATTN J.B. CLADIS DEPT 52-12

MARTIN MARIETTA CORP
ORLANDO DIVISION
P.O. BOX 5837
ORLANDO, FL 32805
  01CY ATTN R. HEFFNER

M.I.T. LINCOLN LABORATORY
P.O. BOX 73
LEXINGTON, MA 02173
  01CY ATTN DAVID M. TOWLE
  01CY ATTN L. LOUGHLIN
  01CY ATTN D. CLARK

MCDONNEL DOUGLAS CORPORATION
5301 BOLSA AVENUE
HUNTINGTON BEACH, CA 92647
01CY ATTN N. HARRIS
01CY ATTN J. MOULE
01CY ATTN GEORGE MROZ
01CY ATTN W. OLSON
01CY ATTN R.W. HALPRIN
01CY ATTN TECHNICAL LIBRARY SERVICES

MISSION RESEARCH CORPORATION
735 STATE STREET
SANTA BARBARA, CA 93101
01CY ATTN P. FISCHER
01CY ATTN W.F. CREVIER
01CY ATTN STEVEN L. GUTSCHE
01CY ATTN R. BOGUSCH
01CY ATTN R. HENDRICK
01CY ATTN RALPH KILB
01CY ATTN DAVE SOWLE
01CY ATTN F. FAJEN
01CY ATTN M. SCHEIBE
01CY ATTN CONRAD L. LONGMIRE
01CY ATTN B. WHITE

MISSION RESEARCH CORP.
1720 RANDOLPH ROAD, S.E.
ALBUQUERQUE, NEW MEXICO 87106
01CY R. STELLINGWERF
01CY M. ALME
01CY L. WRIGHT

MITRE CORPORATION, THE
P.O. BOX 208
BEDFORD, MA 01730
01CY ATTN JOHN MORGANSTERN
01CY ATTN G. HARDING
01CY ATTN C.E. CALLAHAN

MITRE CORP
WESTGATE RESEARCH PARK
1820 DOLLY MADISON BLVD
MCLEAN, VA 22101
01CY ATTN W. HALL
01CY ATTN W. FOSTER

PACIFIC-SIERRA RESEARCH CORP
12340 SANTA MONICA BLVD.
LOS ANGELES, CA 90025
01CY ATTN E.C. FIELD, JR.

PENNSYLVANIA STATE UNIVERSITY
IONOSPHERE RESEARCH LAB
318 ELECTRICAL ENGINEERING EAST
UNIVERSITY PARK, PA 16802
(NO CLASS TO THIS ADDRESS)
01CY ATTN IONOSPHERIC RESEARCH LAB

PHOTOMETRICS, INC.
4 ARROW DRIVE
WOBURN, MA 01801
01CY ATTN IRVING L. KOFSKY

PHYSICAL DYNAMICS, INC.
P.O. BOX 3027
BELLEVUE, WA 98009
01CY ATTN E.J. FREMOUW

PHYSICAL DYNAMICS, INC.
P.O. BOX 10367
OAKLAND, CA 94610
ATTN A. THOMSON

R & D ASSOCIATES
P.O. BOX 9695
MARINA DEL REY, CA 90291
01CY ATTN FORREST GILMORE
01CY ATTN WILLIAM B. WRIGHT, JR.
01CY ATTN ROBERT F. LELEVIER
01CY ATTN WILLIAM J. KARZAS
01CY ATTN H. ORY
01CY ATTN C. MACDONALD
01CY ATTN R. TURCO
01CY ATTN L. DeRAND
01CY ATTN W. TSAI

RAND CORPORATION, THE
1700 MAIN STREET
SANTA MONICA, CA 90406
01CY ATTN CULLEN CRAIN
01CY ATTN ED BEDROZIAN

RAYTHEON CO.
528 BOSTON POST ROAD
SUDBURY, MA 01776
01CY ATTN BARBARA ADAMS

RIVERSIDE RESEARCH INSTITUTE
330 WEST 42nd STREET
NEW YORK, NY 10036
01CY ATTN VINCE TRAPANI

SCIENCE APPLICATIONS, INC.
1150 PROSPECT PLAZA
LA JOLLA, CA 92037
01CY ATTN LEWIS M. LINSON
01CY ATTN DANIEL A. HAMLIN
01CY ATTN E. FRIEMAN
01CY ATTN E.A. STRAKER
01CY ATTN CURTIS A. SMITH
01CY ATTN JACK MCDOUGALL

SCIENCE APPLICATIONS, INC
1710 GOODRIDGE DR.
MCLEAN, VA 22102
ATTN: J. COCKAYNE

SRI INTERNATIONAL
333 RAVENSWOOD AVENUE
MENLO PARK, CA 94025
01CY ATTN DONALD NEILSON
01CY ATTN ALAN BURNS
01CY ATTN G. SMITH
01CY ATTN R. TSUNODA
01CY ATTN DAVID A. JOHNSON
01CY ATTN WALTER G. CHESNUT
01CY ATTN CHARLES L. RINO
01CY ATTN WALTER JAYE
01CY ATTN J. VICKREY
01CY ATTN RAY L. LEADABRAND
01CY ATTN G. CARPENTER
01CY ATTN G. PRICE
01CY ATTN R. LIVINGSTON
01CY ATTN V. GONZALES
01CY ATTN D. MCDANIEL

TECHNOLOGY INTERNATIONAL CORP
75 WIGGINS AVENUE
BEDFORD, MA 01730
01CY ATTN W.P. BOQUIST

TOYON RESEARCH CO.
P.O. Box 6890
SANTA BARBARA, CA 93111
01CY ATTN JOHN ISE, JR.
01CY ATTN JOEL GARBARINO

TRW DEFENSE & SPACE SYS GROUP
ONE SPACE PARK
REDONDO BEACH, CA 90278
01CY ATTN R. K. PLEBUCH
01CY ATTN S. ALTSCHULER
01CY ATTN D. DEE
01CY ATTN D/ STOCKWELL
SNTF/1575

VISIDYNE
SOUTH BEDFORD STREET
BURLINGTON, MASS 01803
01CY ATTN W. REIDY
01CY ATTN J. CARPENTER
01CY ATTN C. HUMPHREY